Available online at www.sciencedirect.com

ScienceDirect

Mendeleev Commun., 2017, **27**, 382–384

Mendeleev Communications

Galvanic displacement of silver deposited on carbon nanowalls by palladium and the electrocatalytic behavior of the resulting composite

Yurii M. Maksimov,[a] Boris I. Podlovchenko,*[a] El'dar M. Gallyamov,[a] Sarkis A. Dagesyan,[b] Vasiliy V. Sen[b] and Stanislav A. Evlashin[b]

[a] *Department of Chemistry, M. V. Lomonosov Moscow State University, 119991 Moscow, Russian Federation. Fax: +7 495 939 0171; e-mail: podlov@elch.chem.msu.ru*

[b] *D. V. Skobeltsyn Institute of Nuclear Physics, M. V. Lomonosov Moscow State University, 119991 Moscow, Russian Federation*

DOI: 10.1016/j.mencom.2017.07.021

The composites $Pd^0(Ag)$, which are highly active in formic acid electrooxidation, were synthesized by galvanic displacement and electrochemical leaching.

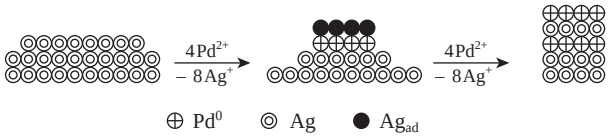

Methods of enhancing the efficiency of palladium in catalysts in direct formic acid fuel cells (improving voltammetric characteristics, decreasing Pd consumption and increasing stability) are of current interest. One of them is based on the use of two-component structures employing a cheap non-noble (or less noble) metal as the second component. Recently, attention was focused on Pd–Ag composites[1–5] because PdAg alloys are the efficient catalysts of formic acid dehydrogenation.[6,7] However, information on the effect of Ag additions on the electrocatalytic activity of Pd catalysts is controversial.[1–5]

Galvanic displacement (GD) and electrochemical leaching are the main electrochemical methods used for the synthesis and modification of Pd–Ag composites.[2–5,8] Earlier,[9,10] we found that carbon nanowalls (CNWs) are convenient model supports for studying nanostructured Pt–Cu and Pt–Bi mixed catalysts. In these studies, we used the GD of Cu and Bi from their layers deposited by magnetron sputtering. It was interesting to use CNW and to apply magnetron sputtering to the Pd–Ag system. In this work, we studied (i) the GD of silver sputtered on CNW by palladium, (ii) the effect of electrochemical leaching on the behavior of the resulting $Pd^0(Ag)$ composite and (iii) the electrocatalytic activity of these catalysts in formic acid oxidation reaction (FAOR).†

The SEM image [Figure 1(*a*)] showed that the sputtered Ag deposit was uniformly distributed over carbon nanowalls to form prolonged 'worms' ~300 nm in diameter. After the displacement of Ag by Pd [Figure 1(*b*)], the 'worms' decreased only a little in length and retained their diameter. This is unexpected because the displacement proceeds in a ratio of 1 Pd atom to 2 Ag atoms and palladium is denser than silver (12 and 10.5 g cm^{-3}, respectively). This effect is apparently associated with an increase in the deposit porosity. After the first potential cycle, the deposit retained its form [Figure 1(*c*)] but became still looser. After three potential cycles, only a small amount of the deposit was retained and the original conglomerates disintegrated to small particles [Figure 1(*d*)]. Moreover, the CNW plates of the support became visible.

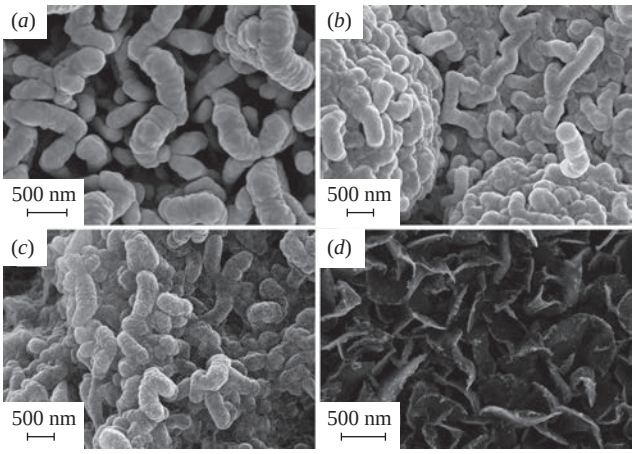

Figure 1 SEM images: (*a*) e.d. Ag, (*b*) $Pd^0(Ag)_{in}$, (*c*) $Pd^0(Ag)_{[1]}$, and (*d*) $Pd^0(Ag)_{[3]}$.

† The study was carried out in a three-electrode cell with separate cathodic and anodic compartments at 20±1 °C; a reversible hydrogen electrode (RHE) in a supporting electrolyte (0.5 M H_2SO_4) solution was used as the reference electrode. The original working electrode represented a glassy carbon plate (S_{geom} = 1 cm^2) modified with CNW,[9–11] on which the Ag layer was deposited by magnetron sputtering (~400 μg per cm^2 of geometrical surface). This electrode was brought into contact with a deaerated 0.5 M H_2SO_4 + 0.001 M $PdSO_4$ solution and the transient of open-circuit potential was recorded up to the establishment of a stationary value (the stationarity criterion was $dE/d\tau < 0.3$ mV min^{-1}). The composite synthesized by the displacement of silver by palladium [designated as $Pd^0(Ag)_{in}$] was washed with twice distilled water and/or a supporting electrolyte solution and studied *ex situ* [SEM, X-ray microprobe analysis (MPA), AES-ICP and XPS] and *in situ* (transients of open-circuit potential, CVA, stationary polarization curves). SEM and MPA measurements were carried out on a JEOLCM-6490LV setup and by means of an NCA X-Sight Oxford Instruments attachment for microprobe analysis; the XPS spectra were recorded on an Axis Ultra DLD spectrometer (Krafos). The electrochemically active surface area (EASA) was determined with respect to copper adatoms.[5] Similar studies were carried out for $Pd^0(Ag)$ samples prepared by the *n*-fold potential cycling of $Pd^0(Ag)_{in}$ in a range of 90–1400 mV (designated as $Pd^0(Ag)_{[n]}$). The polarization curves in a 0.5 M H_2SO_4 + 0.5 M HCOOH solution were recorded in the potentiostatic mode; the current variations by less than 2% per minute were taken as the stationarity criterion.

Table 1 The Ag/Pd ratio in the bulk (according to MPA data) and on the surface (according to XPS data) of $Pd^0(Ag)_{in}$, $Pd^0(Ag)_{[1]}$ and $Pd^0(Ag)_{[3]}$ samples.

$Pd^0(Ag)$ composite	In the bulk		On the surface	
	Ag (at%)	Pd (at%)	Ag (at%)	Pd (at%)
$Pd^0(Ag)_{in}$	78.9	21.1	62	38
$Pd^0(Ag)_{[1]}$	51.6	48.4	28	72
$Pd^0(Ag)_{[3]}$	27.6	72.4	29	71

According to MPA (Table 1), under the conditions used (T = = 20±1 °C, τ = 100 min and $[Pd^{2+}] = 10^{-3}$ mol dm^{-3}), the degree of silver displacement was ~23% (we took into account in the calculations that the displacement proceeds in the ratio Ag : Pd = = 2 : 1). After the first cycle, the silver fraction in the $Pd^0(Ag)_{[1]}$ deposit sharply decreased, which already pointed to the absence of Pd shell capable of preventing the silver dissolution. In the further cycles, Ag continued to dissolve preferentially.

The transient of open-circuit potential corresponding to the process of Ag displacement by Pd (the upper insert in Figure 2) has the form strongly different from that of transients observed at the displacement of Cu layers on CNW by platinum.[12] In the *E vs*. τ curve, the regions where the potential of the Ag–Pd system is determined by the Ag – e ↔ Ag^+ equilibrium, the variation of the electrode total charge[13,14] and the beginning of oxygen adsorption are poorly separated. The found stationary potential was ~770 mV, which substantially exceeds the equilibrium potential of the Ag^+/Ag pair for the Ag^+ concentration established in our system due to displacement of Ag [$E_{eq}^{Ag^+/Ag}$ ~550 mV (RHE)], and is more than 100 mV lower than the equilibrium potential of the Pd^{2+}/Pd pair [~900 mV (RHE)]. The inhibition of the reaction $2Ag + Pd^{2+} \rightarrow Pd^0 + 2Ag^+$ is explained by the beginning of oxygen adsorption on Pd.

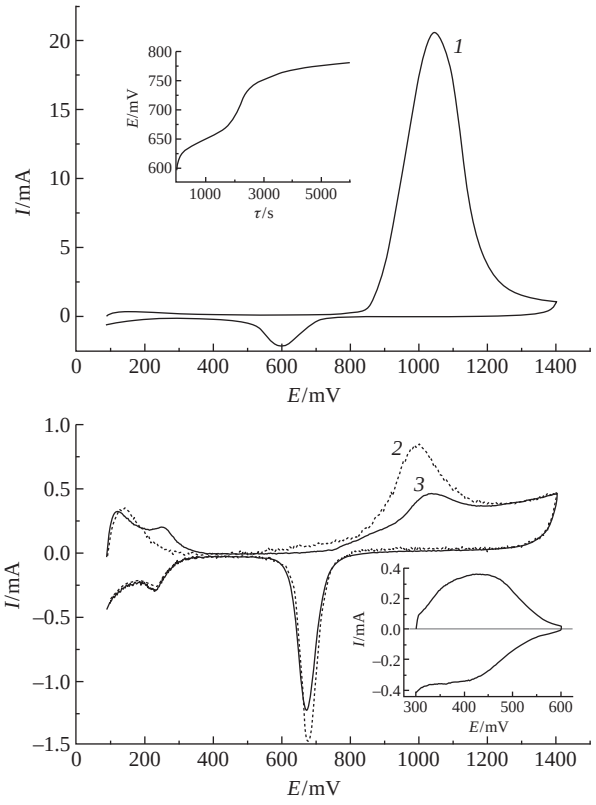

Figure 2 CVA of $Pd^0(Ag)$ in 0.5 M H_2SO_4: (*1*) 1st, (*2*) 2nd, and (*3*) 3rd cycles of potential. Upper insert: transient of open current potential at the contact of e.d. Ag/CNW with 1×10^{-3} M $PdSO_4$ + 0.5 M H_2SO_4. Lower insert: CVA of $Pd^0(Ag)_{[1]}$ in 0.5 M H_2SO_4 + 0.002 M $CuSO_4$. v = 20 mV s^{-1}.

The anodic branch of the $Pd^0(Ag)_{in}$ CVA (Figure 2, curve *1*) demonstrates a very high current mainly corresponding to Ag ionization. This confirms the absence of any sufficiently dense Pd shell. For $Pt^0(Cu)_{in}$ composites, virtually no Cu ionization occurred even in the first CVA cycle.[12] The anodic peak integration of curve *1* gives the quantity of electricity corresponding to the ionization of about a half of the initial Ag deposit. In the second and third potential cycles, the ionization of Ag continues progressively but is less intense. The analysis of solutions (AES-ICP) also demonstrated the weak dissolution of Pd at electrode potential cycling (from ~4 μg in the first cycle to ~1 μg in the second and third cycles). The rough estimate shows that, even after three cycles, the overall mass of the deposit decreases by a factor of ~7, which agrees with the SEM data for $Pd^0(Ag)_{[3]}$ [Figure 1(*d*)].

Figure 2 (lower insert) shows a typical CVA for $Pd^0(Ag)$ composites in 0.5 M H_2SO_4 + 0.002 M $CuSO_4$ (with a 100-s delay at 300 mV in order to form the Cuad monolayer[5,12]). Its form differs from that of the analogous curve measured on electrodeposited (e.d.) Pd, which points to the presence of noticeable amounts of Ag on the surface of all samples.[5] Calculations of EASA with respect to Cu_{ad} gave the values of 8.8, 7.8 and 3.3 cm^2 for $Pd^0(Ag)_{in}$, $Pd^0(Ag)_{[1]}$ and $Pd^0(Ag)_{[3]}$, respectively. Previously,[5] it was found that the copper adsorption on silver can be neglected, *i.e.*, the obtained EASA values correspond to the surface of the Pd component only. Based on the data on the Pd content of $Pd^0(Ag)_{in}$, the specific EASA of this sample was determined to be ~25 m^2 g^{-1} Pd, which indicates the high degree of Pd dispersion in $Pd^0(Ag)_{in}$. Assessing the surface composition of the three $Pd^0(Ag)$ samples based on the overall XPS spectra (Table 1) showed that, immediately after the displacement, the surface layer of $Pd^0(Ag)_{in}$ contained the double amount of Pd, as compared with the deposit bulk. The substantial enrichment of the surface layer with Pd proceeds after the removal of Ag in the first potential cycle [Table 1, $Pd^0(Ag)_{[1]}$]; however, in the next cycles, the surface layer composition does not change noticeably; moreover, after the third cycle, it approaches the bulk composition. Although the depth of XPS analysis (3–4 nm) corresponds to more than 10 monolayers of the PdAg alloy (r_{Pd} = 0.137 nm, r_{Ag} = 0.144 nm), the high Ag content of the analyzed layer makes improbable its presence in 1–2 upper monolayers in only insignificant amounts. This convincingly follows from the electrochemical data, which characterize *in situ* the uppermost layer. For comparison, note that the XPS data confirmed the presence of <2 at% Cu in the surface layer for the formation of a dense Pt shell on copper.[12]

Pd and Ag have the same lattice type (fcc) with close parameters [a(Pd) = 0.3890 and a(Ag) = 0.4086 nm]. This is a good prerequisite for the formation of a sufficiently dense shell upon the contact of Pd^{2+} ions with silver.[5,15] However, the above results clearly demonstrate the absence of formation of such a shell. Why this happens? From our point of view, the main reason is the fact that silver adatoms (Ag_{ad}) block a considerable part of Pd^0 formed at GD. The potential region in which the GD proceeds (~600–800 mV) coincides with the potential region of the irreversible adsorption of Ag^+ ($Ag^+ + e \rightarrow Ag_{ad}$).[16] Ag_{ad} can be removed from the Pd surface only at the oxygen adsorption potentials.[16] This is why, being formed on the Pd^0 surface, they are not displaced by Pd but are incorporated into the shell. In contrast to Ag_{ad}, the Cu_{ad} adatoms are desorbed in the potential region of the electric double layer both from Pt and from Pd (*i.e.*, before the oxygen adsorption starts), which determines the main difference observed at the GD of Ag and Cu layers. The incorporation of Ag_{ad} into the $Pd^0(Ag)_{in}$ shell is shown in Figure 3.

Note that neither the formation of Ag_{ad} (first step) nor the transition of Ag_{ad} into a silver metal phase (second step) need electricity consumption because the charge of Ag_{ad} is zero.

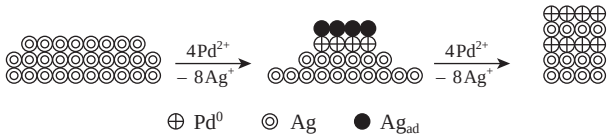

Figure 3 The incorporation of Ag_{ad} into the $Pd^0(Ag)_{in}$ shell.

The attempt of further enrichment of the $Pd^0(Ag)$ surface layer with palladium by electrode potential cycling failed, which is also associated by and large with the above behavior of Ag_{ad}. The fact that the potential cycling resulted in the enrichment of the surface layer of PdAg alloy with Pd (up to ~83 at% according to XPS data) can be explained[5] by the different morphology of deposits and the use of the much larger number of cycles (up to 25) for case of e.d. PdAg alloy. This cannot be applied to $Pd^0(Ag)_{in}$ because the deposit mass is very small and the deposit quickly dissolves on potential cycling.

From the viewpoint of the development of direct formic acid fuel cells, the stationary currents of FAOR in the low potential region are of interest.[5] Figure 4 shows that all $Pd^0(Ag)$ samples demonstrate the higher specific activity (per cm^2 of EASA) in FAOR, as compared with that of e.d. Pd (curve *1*). As we pass from e.d. Pd to $Pd^0(Ag)_{in}$ and $Pd^0(Ag)_{[3]}$, the current *i* increases by factors of ~2 and ~5 at 150 mV or ~1.5 and 6 at 200 mV, respectively. The most probable reason for this is that the Pd atoms and/or clusters present on the surface efficiently block the sites for the formation of strongly chemisorbed species (first of all, CO_{ads}) that usually inhibit the FAOR.[17–21] Furthermore, the formation of new active sites (ensembles) for the direct path of FAOR can occur.[18–20] In both the former and the latter cases, the boundary between Pd and Ag on the electrode surface played an important role.[19,22,23] The latter argument explains the fact that no catalytic effect of Ag on FAOR was observed on e.d. PdAg with ~50 and ~80% Ag contents on the surface,[5] whereas this effect was considerable in $Pd^0(Ag)$ samples with the close surface composition (Table 1, Figure 4).

The degree of Pd utilization in Pd-based catalysts is characterized by the current per Pd mass (A g^{-1} Pd). The rough estimates of this current for $Pd^0(Ag)$ composites at 200 mV are ~5.5 and ~9 A g^{-1} for $Pd^0(Ag)_{in}$ and $Pd^0(Ag)_{[3]}$, respectively, which are higher by factors of ~2 and ~4, respectively, than the FAOR currents per Pd mass on highly disperse e.d. Pd at 200 mV.[22]

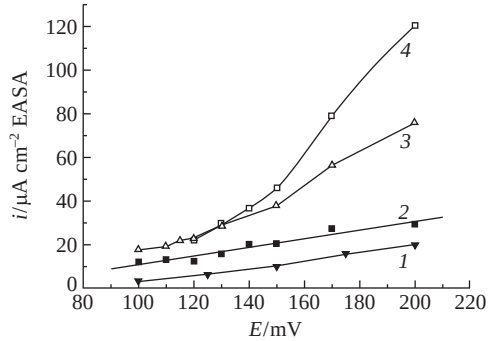

Figure 4 Stationary polarization curves in 0.5 M HCOOH + 0.5 M H_2SO_4 solution on (*1*) e.d. Pd, (*2*) $Pd^0(Ag)_{in}$, (*3*) $Pd^0(Ag)_{[1]}$, and (*4*) $Pd^0(Ag)_{[3]}$ (support, CNW).

This work was supported by the Russian Foundation for Basic Research (project nos. 15-03-03436A and 17-08-01414A), the Scholarship of the President of the Russian Federation (grant no. SP-1493.2016.4) and in part by the M. V. Lomonosov Moscow State University Program of Development.

References

1 S. Hu, L. Scudiero and S. Ha, *Electrochem. Commun.*, 2014, **38**, 107.
2 Y. Yang, W. Wang, Y. Liu, F. Wang, Z. Zhang and Z Lei, *Int. J. Hydrogen Energy*, 2015, **40**, 2225.
3 D. Chen, P. Cui, H. Liu and J. Yang, *Electrochim. Acta*, 2015, **153**, 461.
4 Y. Tong, X. Lu, W. Sun., G. Nie, L. Yang and C. Wang, *J. Power Sources*, 2014, **261**, 221.
5 B. I. Podlovchenko, Yu. M. Maksimov and A. G. Utkin, *Russ. J. Electrochem.*, 2015, **51**, 891 (*Elektrokhimiya*, 2015, **51**, 1011).
6 K. Tedsree, T. Li, S. Jones, C. W. A. Chan, K. M. K. Yu, P. A. J. Bagot, E. A. Marquis, G. D. W. Smith and S. C. E. Tsang, *Nat. Nanotechnol.*, 2011, **6**, 302.
7 J. Liu, L. Lan, R. Li, X. Liu and C. Wu, *Int. J. Hydrogen Energy*, 2016, **41**, 951.
8 C.-W. Chen, Y.-S. Hsieh, C.-C. Syu, H.-R. Chen and C.-L. Lee, *J. Alloys Compd.*, 2013, **580**, S359.
9 B. I. Podlovchenko, V. A. Krivchenko, Yu. M. Maksimov, T. D. Gladysheva, L. V. Yashina, S. A. Evlashin and A. A. Pilevsky, *Electrochim. Acta*, 2012, **76**, 137.
10 B. I. Podlovchenko, Yu. M. Maksimov, S. A. Evlashin, T. D. Gladysheva, K. I. Maslakov and V. A. Krivchenko, *J. Electroanal. Chem.*, 2015, **743**, 93.
11 V. A. Krivchenko, Yu. M. Maksimov, B. I. Podlovchenko, A. T. Rakhimov, N. V. Suetin and M. A. Timofeev, *Mendeleev Commun.*, 2011, **21**, 264.
12 B. I. Podlovchenko, T. D. Gladysheva, A. Yu. Filatov and L.V. Yashina, *Russ. J. Electrochem.*, 2010, **46**, 1189 (*Elektrokhimiya*, 2010, **46**, 1272).
13 A. N. Frumkin, *Potentsialy nulevogo zaryada (Zero-Charge Potentials)*, Nauka, Moscow, 1981 (in Russian).
14 B. I. Podlovchenko and E. A. Kolyadko, *J. Electroanal. Chem.*, 2001, **506**, 11.
15 J. H. Koh, R. Abbaraju, P. Parthasarathy and A. V. Virkar, *J. Power Sources*, 2014, **261**, 271.
16 B. I. Podlovchenko and E. A. Kolyadko, *J. Electroanal. Chem.*, 1987, **224**, 225.
17 R. P. Petukhova, G. Garson Valensiya and B. I. Podlovchenko, *Vestn. Mosk. Univ., Ser. Khim.*, 1987, **28**, 62 (in Russian).
18 M. Neurock, M. Janik and A. Wieckowski, *Faraday Discuss.*, 2009, **140**, 363.
19 B. I. Podlovchenko and Yu. M. Maksimov, *J. Electroanal. Chem.*, 2015, **756**, 140.
20 Y. X. Chen, S. Ye, M. Heinen, Z. Jusus and R. J. Behm, *Langmuir*, 2006, **22**, 10399.
21 J. V. Perales-Rondón, E. Herrero and J. M. Feliu, *J. Electroanal. Chem.*, 2015, **742**, 90.
22 T. D. Gladysheva, A. Yu. Filatov and B. I. Podlovchenko, *Mendeleev Commun.*, 2015, **25**, 56.
23 T. D. Gladysheva, B. I. Podlovchenko, D. S. Volkov and A. Yu. Filatov, *Mendeleev Commun.*, 2016, **26**, 298.

Received: 2nd November 2016; Com. 16/5088